The thermodynamics of electrochemical annealing

Margret Giesen, Guillermo Beltramo, Sabine Dieluweit, Jorge Müller, Harald Ibach

Institute of Thin Films and Interfaces, Research Center Jülich, 52425 Jülich, Germany

Wolfgang Schmickler

Abteilung Elektrochemie, Universität Ulm, D-89069 Ulm, Germany

Abstract:

We show that on solid electrodes held at constant potential in an electrolyte all defect formation energies and activation energies for surface transport become potential dependent. The rapid smoothening of rough metal electrodes for (mostly) positive electrode potentials ("electrochemical annealing") is therefore the consequence of the specific thermodynamic boundary condition of constant electrode potential. The potential dependence can be related to the surface charge density and the dipole moments of the defects. With dipole moments calculated by ab-initio methods the theory is applied to experimental data on two-dimensional Ostwald-ripening on Au(100) electrodes. The theory is further discussed in the context of other experiments.

Keywords: Ab-initio quantum chemical methods and calculations, models of surface kinetics, thermodynamics, electrochemical methods, scanning tunneling microscopy, surface diffusion, gold.

1. Introduction

Classical electrochemical reactions involve the transfer of charged particles through the interface between an electrode and an electrolyte solution. The driving force for such reactions is the product of the charge on the particle and the difference in the electrostatic potential across the interface, which is proportional to the electrode potential. The reaction rates depend exponentially on the electrode potential, since the energies of activation vary linearly with the driving force – a principle known as a linear free energy relation in chemical kinetics. The advent of the electrochemical scanning tunneling microscope (STM) has made it possible to investigate processes that occur on the electrode surface itself and *do not* involve the transfer of charge *across* the interface. Examples are the diffusion of single adatoms or vacancies, their generation from kink sites, and the interlayer transport of atoms. Since the initial and final states of such processes are both on the surface, their driving force is not directly affected by the electrode potential. Nevertheless, the rates of many coarsening phenomena, which involve a combination of the processes listed above, have been found to depend exponentially on the potential. In most cases, the rate grows as the potential is raised towards more positive values. The thereby induced smoothening of the surface has been termed “electrochemical annealing” [1] in order to stress the apparent similarity between the effect of the potential and a raise in temperature. To our knowledge, the first quantitative investigations on electrochemical annealing concern the smoothening of rough gold and platinum electrodes [2-4]. More recently, the filling of STM-induced indentations and the decay of deposited islands were studied on Ag(100) and Au(100) electrodes [5-7]. Quantitative investigations on structurally well-defined systems include equilibrium fluctuations of monatomic steps on Cu and Ag surfaces [8-11]. All studies report an approximately exponential increase of the rate of transport processes with the electrode potential. Considering the very different nature of the investigated processes, which involve different combinations of atomic processes with different activation energies we conclude that there should be a common, rather general cause for the exponential dependence, irrespective of the specific process, surface, and electrolyte. We show that the common cause rests in the thermodynamic conditions of charged electrolyte surfaces held at constant potential. Because of this thermodynamic constraint, all defect formation energies are renormalized by an electrostatic energy term that involves the difference in charge density on surfaces with and without defects. The same arguments apply to activation energies for surface transport process. There, the electrostatic term involves the difference in the charge density on a surface with defects in the

activated state and a surface with defect in the ground state. As charge densities are to first order linear in the potential, the exponential dependence of transport rates on the potential finds a natural and general explanation.

The paper is organized as follows. The general thermodynamic formalism is presented in the next section. Section 3 discusses a simple model for the defect-induced change in the charge density. According to this model, defect formation energies depend linearly on the product of the charge density of the defect-free surface and the dipole moment of the defect. Quantitative aspects of the model are explored with the help of experiments on two-dimensional (2D) Ostwald ripening that are described in Section 4. Section 5 gives a brief account of ab-initio calculations on the dipole moments of defects and on the migration path involved in Ostwald ripening and analyzes the experimental data in the framework of the proposed model. In section 6, we extend the discussion to previously published quantitative experimental data.

2. The potential dependence of defect energies

The thermodynamics of electrode surfaces in an electrolyte differs from the thermodynamics of surfaces in vacuum because of the constraint of constant electrode potential. The correct thermodynamic potential for the surface energy, the surface tension γ, defined as the work per area required for generating a surface is

$$\gamma = f_s + \sigma \frac{\partial f_s}{\partial \sigma} \equiv f_s - \sigma\phi \qquad (1)$$

in which f_s is the area specific free energy, σ is the area specific surface charge [12] and ϕ is the electrode potential on the vacuum scale. Free surface energy and surface tension coincide only for uncharged surfaces. Under the boundary condition of constant ion concentrations in the electrolyte and constant temperature, the surface tension can be expressed in terms of the potential dependence of the surface charge density $\sigma(\phi)$

$$\gamma(\phi) = \gamma_{pzc} - \int_{\phi_{pzc}}^{\phi} \sigma(\phi')d\phi' \qquad (2)$$

Here γ_{pzc} and ϕ_{pzc} denote the surface tension and the potential at zero charge. From eq. (2) follows that the surface tension γ has a maximum at the potential of zero charge (pzc) [13], which is a well known fact in electrochemistry. For the understanding of the following considerations it is

important to note that $\sigma(\phi)$ is the macroscopically *measured* charge density, not the *true* charge density on the electrode surface that one might consider in ab-initio calculations. For example, the charge in eq. (2) includes the charge that is macroscopically unloaded on the electrode during specific adsorption of ions from the electrolyte.

We expand these considerations to the thermodynamics of defect generation and migration. The work required to generate the defect on an electrode surface held at constant potential E_{def} is the difference in the surface tension per defect for a surface with defects, γ_{def}, and without the defects, γ_0, hence

$$E_{def}(\phi) = \lim_{\rho \to 0} \frac{1}{\rho} \left\{ \gamma_{def}(\phi) - \gamma_0(\phi) \right\}. \qquad (3)$$

in which ρ is the density of defects on the surface. With the help of eq. (2), one can express the surface tensions in terms of the charge densities of the surface with and without the defects.

$$E_{def}(\phi) = E^{o}_{def} - \lim_{\rho \to 0} \frac{1}{\rho} \left\{ \int_{\phi_{pzc,0}}^{\phi} (\sigma_{def}(\phi') - \sigma_0(\phi'))\, d\phi' + \int_{\phi_{pzc,def}}^{\phi_{pzc,0}} \sigma_{def}(\phi')\, d\phi' \right\} \qquad (4)$$

Here, E^{0}_{def} is the work required to create a defect on uncharged surfaces. This part of the formation energy is the analogue of the defect formation energy on a surface in vacuum held at constant (= zero) charge. $\phi_{pzc,0}$ and $\phi_{pzc,def}$ are the potentials of zero charge on the defect free surface and the surface with defects. The pzc of the surface with and without defects differ because defects carry a dipole moment μ_{def}. This dipole moment causes a shift in the work function. The work function is reduced when the dipole moment is positive, i.e. points with its positive end towards vacuum/electrolyte. The change of the work function is equivalent to a change in the pzc [13]. The magnitude of the shift is

$$\Delta\phi \equiv \phi_{pzc,0} - \phi_{pzc,def} = \rho \mu_{def} / \varepsilon_0 \qquad (5)$$

Here, $\phi_{pzc,0}$ and $\phi_{pzc,def}$ denote the pzc of the surface without and with the defects, ρ is the defect concentration and ε_0 the vacuum permittivity. The second integral in eq. (4) extends from $\phi_{pzc,def}$ to $\phi_{pzc,def}+\Delta\phi$. Its value is proportional $(\Delta\phi)^2$, and therefore proportional to ρ^2 (eq. (5)). It vanishes in the limit $\rho \to 0$. The work required to generate a defect at the solid electrolyte interface held at constant potential is therefore

$$E_{def}(\phi) = E_{def}^{0} - \lim_{\rho \to 0} \frac{1}{\rho} \left\{ \int_{\phi_{pzc,0}}^{\phi} (\sigma_{def}(\phi') - \sigma_0(\phi'))\, d\phi' \right\} \qquad (6)$$

Hence, the potential dependence of the defect formation energy is given by the integral over the difference in the charge densities on a surface with and without the defects, $\sigma_{def}(\phi)$-$\sigma_0(\phi)$. Analog to eq. (6) one has for the activation energy for atom transport on surfaces

$$E_{act}(\phi) = E_{def}^{0} - \lim_{\rho \to 0} \frac{1}{\rho} \left\{ \int_{\phi_{pzc,0}}^{\phi} (\sigma_{def}^{+}(\phi') - \sigma_{def}(\phi'))\, d\phi' \right\} \qquad (7)$$

with $\sigma_{def}^{+}(\phi)$ the charge density on a surface with defects in the activated transition state. We note that no approximation is made in the derivation of eqs. (6) and (7).

According to Eqs. (6) and (7) all formation energies and activation energies are potential dependent. As these equations are derived from the specific form of the surface tension for electrode surfaces held at constant potential in an electrolyte, the potential dependence of the defect formation energies and activation energies is also a consequence of the thermodynamic boundary condition of constant potential. In essence, one may say that because of this condition the power supply keeping the electrode potential constant contributes to the defect formation energies and activation energies for transport.

Without loss of generality, we can expand the surface charge densities around a particular potential ϕ_0

$$\sigma_{def}(\phi) = \sigma_{def}(\phi_0) + C_{def}(\phi_0)(\phi - \phi_0)... \qquad (8)$$

$$\sigma_0(\phi) = \sigma_0(\phi_0) + C_0(\phi_0)(\phi - \phi_0)... \qquad (9)$$

in which $C_{def}(\phi_0)$ and $C_0(\phi_0)$ are the differential capacitances of the surface with and without defects. Inserting eqs. (8) and (9) into eq. (6), one obtains the expansion

$$E_{def}(\phi) = E_{def}(\phi_0) - \lim_{\rho \to 0} \frac{1}{\rho} \left\{ \left[\sigma_{def}(\phi_0) - \sigma_0(\phi_0)\right](\phi - \phi_0) + \frac{1}{2}\left[C_{def}(\phi_0) - C_0(\phi_0)\right](\phi - \phi_0)^2 ... \right\} . \qquad (10)$$

In a small potential range, the defect energies are therefore a linear function of the potential. The same holds for activation energies for transport processes. In experiments, one is therefore bound to find potential regions where the rates depend exponentially on the electrode potential,

provided that the charge density differences that enter into the energies are large enough to create a noticeable effect.

3. Charge density on surfaces with defects

In order to calculate defect formation energies and activation energies one needs the charge densities as a function of the potential. The charge density of the defect free surface $\sigma_0(\phi)$ is easily measured according to standard procedures in electrochemistry. The experimental determination of the charge density on a surface with defects $\sigma_{def}(\phi)$ requires the preparation of a surface with a defined and a not too small concentration of the defects considered. This is possible for steps since surfaces with a defined concentration of steps can be prepared by cutting crystals in an orientation vicinal to a low index plane. The potential dependence of the step line tension is therefore amenable to experimental determination. Experiments along this direction are currently in progress and will be reported shortly [14]. For other defects, e.g. for adatoms or vacancies on terraces $\sigma_{def}(\phi)$ must be taken from theory. It is at present not possible to calculate the charge density on surfaces in an electrolyte by ab-initio methods, since the theory would have to take the solid, the inner Helmholtz layer and the liquid electrolyte into account. It is however possible to consider various contributions to the charge density and relate these contributions to other physical quantities.

The charge density on an electrode surface at a particular potential ϕ_0 has three conceptually distinct contributions. One arises from the position of the potential of zero charge. The larger the difference between ϕ_0 and ϕ_{pzc} the larger is the charge. A shift in the pzc due to the presence of defects therefore contributes to the relevant charge density difference in eq. (6). The magnitude of the contribution is proportional to the dipole moment of the defect (eq. (5)). We illustrate the point with the help of a measured charge density on the Au(100) surface in a 50 mM H_2SO_4 electrolyte in Fig. 1 (solid line). The pzc is near 0V vs. the saturated calomel electrode (SCE). The hump at around 50 mV SCE is due to the onset of specific adsorption of ions, which we discuss in detail later. Suppose that the surface has a particular concentration of defects. By virtue of their dipole moment the pzc would change according to eq. (5), and therefore the entire charge density curve would also shift (dashed line). The charge density on the surface with defects can then be written as

$$\sigma_{def}(\phi) = \sigma_0(\phi + \Delta\phi) = \sigma_0(\phi) + \frac{\partial\sigma_0}{\partial\phi}\Delta\phi + \frac{1}{2}\frac{\partial^2\sigma_0}{\partial\phi^2}(\Delta\phi)^2 \ldots \qquad (11)$$

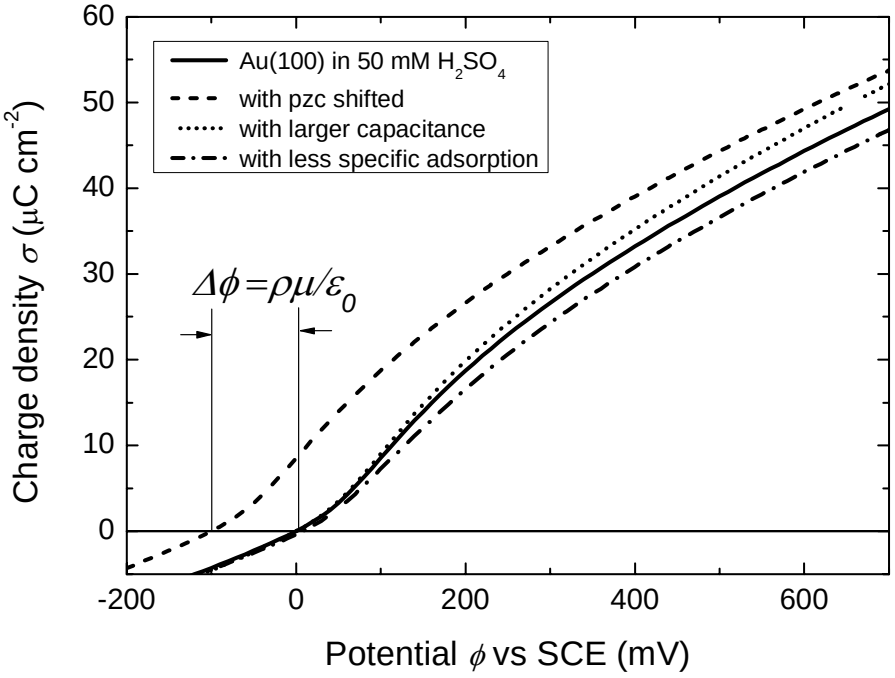

Fig. 1: The measured surface charge density as a function of the electrode potential for the unreconstructed Au(100)-surface in 50 mM H_2SO_4 (solid line) together with various model charge densities for the surface with defects (dashed, dotted and dash-dotted lines, see text for discussion).

The third term is proportional to ρ^2 and vanishes in the limit $\rho \to 0$. After inserting eq.(11) together with eq. (5) into eq. (6) one obtains the remarkable simple equation for the potential dependence of the defect formation energy due to the shift in the pzc

$$E_{def}(\phi) = E^0_{def} - \frac{\mu_{def}}{\varepsilon_0}\sigma_0(\phi)\,. \qquad (12)$$

The same type of equation applies to the energy of a defect in an activated state, e.g. in the transition state for diffusion. The activation energy for the diffusion therefore becomes

$$E_{act}(\phi) = E^0_{act} - \frac{\mu^+ - \mu_{def}}{\varepsilon_0}\sigma_0(\phi)\,, \qquad (13)$$

with μ^+ the dipole moment of the defect in the transition state. The extra energy terms in eqs. (12, 13) could be interpreted as the electrostatic energy of a dipole in an electric field σ_0/ε_0. There is

the caveat however, that σ_0 is not the microscopic electric charge density on the electrode but the macroscopically charge density that has flown in the external circuit (see above). By virtue of the extra energy terms in eqs. (12, 13), all defect formation energies and activation energies involved in surface migration processes would become a linear function of the (macroscopically measured) surface charge density of the defect free surface. In other words, the model predicts that the logarithms of atom transport rates at solid/electrolyte interfaces should depend linearly on the experimentally measured surface charge density, regardless of the nature of the rate-determining step.

So far, we have considered merely the contribution from the shift in the pzc due to defects. A second contribution to the charge density difference in eq. (6) and therefore to the potential dependence of defect energies arises from the change in the Gouy-Chapman capacitance. With reference to Fig. 1 this change in the capacitance would give rise to a different slope of the charge density for the surface with defects (dotted line in Fig. 1). The Gouy-Chapman capacitance on a surface with defects may differ from the surface without defects for two reasons. The first one is that the defects may screen part of the surface, which causes a reduction of the capacitance. This effect has been shown to be rather small [15]. A second cause for a change in the capacitance is that the defects have a different polarizability than the normal surface atoms. Using a self-consistent solution of the Schroedinger-Poisson equation for a metal in the jellium approximation and the Poisson-Boltzmann equation for the electrolyte we have shown that for the case of steps this contribution is also small [12] and has little effect on the charge density of the surface compared to the effect of the shift in pzc. We must leave to future investigation to show whether this result for steps is pertinent to point defects.

A third contribution may arise from specific adsorption of ions. A theoretical analysis would require the calculation of adsorption isotherms for surfaces with and without defects as a function of the potential. A rough estimate for an upper bound on the magnitude of the effect is obtained if one assumes that the surface area covered by the defect, e.g. an adatom or a vacancy is completely blocked for ion adsorption. The change of surface charge is then

$$\sigma_{def}(\phi) - \sigma_0(\phi) = \mp \rho \, \mathrm{e} z \, A_{def} / A_{ion} = \mp \rho \, \mathrm{e} z \, A_{def} \Gamma_{ion}(\phi) \qquad (14)$$

Here, e is the charge of an electron, z is the electrosorption valency, A_{def} and A_{ion} are the areas covered by the defect and the ion, respectively. The area covered by the ion is just the inverse of the surface excess of ions (= number of ions per area). The effect on the charge density caused by

site blocking is illustrated in Fig. 1 by the dash-dotted line. The minus sign in eq. (14) is for the adsorption of negative ions at potentials positive of pzc. The energy per defect is then

$$E_{def}(\phi) = E_{def}^{0} \pm \mathrm{ez}A_{def} \int_{\phi_{pzc}}^{\phi} \Gamma_{ion}(\phi')d\phi' \qquad (15)$$

Here the positive sign is for adsorption of negative ions at potentials positive of pzc, the negative sign for adsorption of positive ions at potentials negative of pzc. The site blocking mechanism leads therefore always to an increase in the defect creation energy. If, alternatively, the specific adsorption on the area covered by the defect would be twice as large as on the normal surface, then the same equation would hold with the sign inverted. Eq. (15) can be used for an estimate of the change in the defect energy due to specific adsorption if the surface excess is known. For the Au(111)-surface e.g. the maximum surface excess for sulfate is $\Gamma_{SO_4^-} = 2.5\times10^{14}$ cm^{-2} [16]. The electrosorption valency is one. Considering the formation energy of an adatom on that surface covering the area $A_{def} = 7.2\times10^{-16}$ cm^2 one obtains

$$E_{def}(\phi) = E_{def}^{0} + 0.18\mathrm{e}(\phi - \phi_{pzc}) \qquad (16)$$

Since a complete blocking of the specific adsorption should be an upper limit of the effect eq.(16) should also be an upper limit on the magnitude of the effect of specific adsorption on defect formation energies.

4. Experiments on Ostwald ripening

In order to study the quantitative aspects of eqs. (6) and (7) we have investigated Ostwald ripening of two-dimensional islands. This experiment is well understood in terms of the participating atomic processes [17-19]. The Au(100) surface represents an ideal system for such studies. By immersing a reconstructed Au(100) electrode into an electrolyte at a potential negative of pzc and subsequently raising the electrode potential, the reconstruction is lifted [20] and the surplus atoms emerge in the overlayer to form two-dimensional adatom islands. The kinetics of this process produces a certain distribution of island sizes (see insert in Fig. 2). In the subsequent ripening process the smaller islands decay in size according to their higher Gibbs-Thomson chemical potential, and the atoms attach to larger islands or steps on the surface. The kinetics of island decay on metal surfaces is controlled either by the attachment/detachment of

the diffusing species from the island edge or by the diffusion on the terraces. The decay curves we observed for adatom islands on Au(100) in H_2SO_4 indicate that the decay is diffusion limited [21], as is typical for adatom mediated transport on surfaces [17, 19, 22]. Transport by single atom vacancies leads to attachment-detachment limited decay [23, 24].

For diffusion-limited decay, the decay rate depends on the environment of the island. If the island is located in the center of a larger vacancy islands, the decay rate of the area A of the center island is [22]

$$\frac{dA}{dt} = \frac{2\pi\nu_0}{\ln(r_o(t)/r_i(t))}\frac{\beta\Omega}{k_BT}\left(\frac{1}{r_i(t)} - \frac{1}{r_o(t)}\right)\exp\left(-\frac{E_{adt}+E_{act}}{k_BT}\right) \qquad (17)$$

Here, $r_i(t)$ and $r_o(t)$ are the radii of the inner island and the outer vacancy island, respectively, ν_0 is the pre-exponential factor for diffusion on the terraces, β is the step line tension, Ω is the area of an atom, E_{adt} and E_{act} are the adatom formation energy and the activation energy for diffusion on terraces, respectively. The minus sign before the term $1/r_o$ occurs because of the negative Gibbs-Thompson chemical potential of the outer vacancy island. The term can be neglected if the center island is in its final stage of decay. Eq. (17) can be solved by numerical integration. If the island under consideration is located inside a wreath of much larger adatom islands (see e.g. the encircled island in the insert of Fig. 2), then the radius of the vacancy island in the logarithmic term is replaced by a time independent mean distance $\langle \mathrm{R} \rangle$ of the outer adatom islands. One then can define a normalized decay rate $\dot{\mathrm{A}}_{\mathrm{norm}}$, which depends only on general parameters, in particular E_{adt} and E_{act} [22]

$$\dot{A}_{norm} = \frac{dA}{dt}r_i(t)\,\ln\left(\langle R\rangle / r_i(t)\right) \propto \exp\left\{-\frac{E_{adt}(\sigma(\phi))+E_{act}(\sigma(\phi))}{k_BT}\right\}. \qquad (18)$$

By plotting the log of the normalized rate during the final decay of an island versus the charge density, one should therefore be able to determine the dependence of the sum of E_{adt} and E_{act} on the charge density and thereby the dependence on the potential.

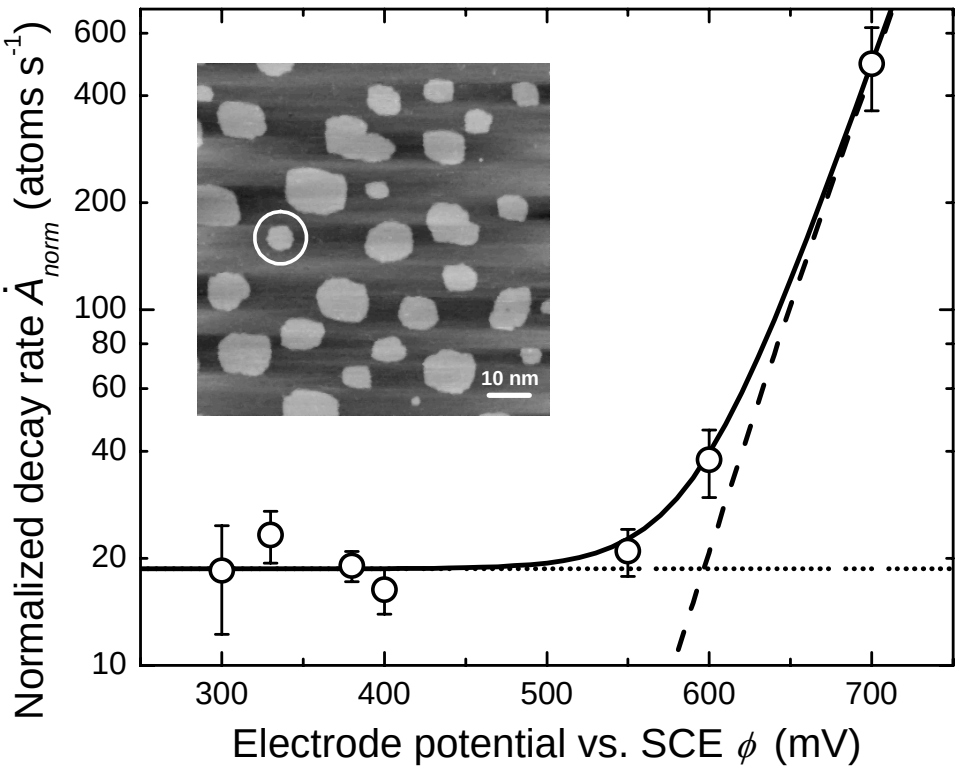

Fig. 2: Normalized decay rate (see text) at room temperature as a function of the electrode potential (with reference to the saturated calomel electrode, SCE). Note the logarithmic scale! The dotted line is the mean of the data points between 300 and 400 mV. The dashed line is calculated in the model when fitted to the data point at 700 mV. The solid curve is the sum of the dotted and dashed line (see text). The insert shows a scanning tunneling microscope image of one atom layer high islands on Au(100) in 50 mM H_2SO_4 produced by the lifting of the reconstruction.

For this purpose we have determined the normalized decay rate on Au(100) in 50 mM H_2SO_4 at 7 different potentials. Details of the experimental conditions are described in [25]. For each potential, decay curves of several islands were measured. The averaged normalized decay rates are shown in Fig. 2 as circles with the standard deviation as error bars. The areas A and radii r_i are normalized to atom areas and atom diameters, respectively. The experimental data show a potential independent decay rate at low potentials and a rapid increase beyond 550 mV. The potential independent normalized decay rate obtained from the data points at 300-400 mV amounts to 19 atoms/s (dotted line).

5. Application of the model to the experimental data

We now discuss the experimental data on Ostwald ripening in terms of the theory developed in Sects. 2 and 3. The exponential term in eq. (18) involves the sum of E_{adt} and E_{act}, which is the energy required to bring one atom from a kink site into the activated transition state of terrace diffusion. We are concerned with this particular energy. We first consider the effect of specific adsorption in view of eq. (16). The site blocking mechanism discussed in Sect. 3 would predict a decrease in the decay rate for increasingly positive potentials at variance with the experiment. In order to explain the observed increase one would have to assume that sulfate atoms adsorb in larger quantities on surfaces with atoms in the activated state. This possibility cannot be dismissed off-hand; however, one has to look at the numbers. For an estimate we assume that the sulfate surface excess on Au(100) is the same as on Au(111). As to the change in the sulfate excess on the surface with atoms in the activated state, we consider the extreme that each atom in the activated state binds twice as many sulfate ions than a normal surface atom. The energy in the activated state would then change by the amount

$$E^{+}(\phi) = E^{+,0} - 0.18\mathrm{e}(\phi - \phi_{pzc}) \tag{19}$$

According to this, the rate would change between 550meV and 700meV by the factor

$$\frac{\dot{A}_{norm}(700\mathrm{mV})}{\dot{A}_{norm}(550\mathrm{mV})} = \mathrm{e}^{\frac{0.18\times 0.15\times 11604}{300}} = 2.84 \tag{20}$$

The experimental ratio is 25. Specific adsorption can therefore not explain the observed rapid increase in the decay rate. Moreover, it hardly contributes any significant amount to this experiment.

We now turn to the effect caused by the shift in pzc. According to eqs. (12) and (13), the energy of the activated state should vary as

$$E^{+}(\phi) = E^{+,0} - \mu^{+}\sigma_0(\phi)/\varepsilon_0 \tag{21}$$

The decay rate should then be described by

$$\ln(\dot{A}_{norm}) = \mu^{+}\sigma_0(\phi)/\varepsilon_0 k_B T + const\,. \tag{22}$$

The charge density was measured according to standard electrochemically techniques and was already plotted in Fig. 1 (solid line). Hence, the dipole moment of the transition state remains the only unknown quantity.

In order to obtain an explicit value for that dipole moment and to further establish the atom migration process as the relevant channel for island decay, we have calculated the migration paths of adatoms and vacancies on an Au(100) surface using the density functional formalism [26]. The calculations include scalar relativistic corrections for the valence electrons and full relativistic cores. We have considered diffusion via vacancies, adatom hopping and adatom exchange diffusion (proposed by Feibelman [27]). The results show that adatom transport with hopping diffusion is the channel with the lowest activation energy (E_{adt}+E_{act} = 1.30eV at pzc) and that this decay is diffusion limited [28]. Hence, the dipole moment to be considered in eq. (22) is that of the transition state for adatom hopping for which we calculate μ^+ = 0.144 eÅ. We note that this dipole moment is quite large. It is about an order of magnitude larger than the dipole moment of step atoms [14, 29, 30].

Using the value for the dipole moment in the activated state μ^+ = 0.144 eÅ and the potential dependence of the measured charge density (Fig. 1) the dashed line in Fig. 2 is calculated. Note that the x-axis in Fig. 2 is the potential not the charge density! The absolute value is fitted to the data point at 700 mV. The theory therefore describes the observed rapid increase of the rate in a small potential range. With a constant term added (dotted line in Fig. 2, representing the mean of the data points between 300 and 400 mV), the rapid increase in the experimentally observed normalized rate is well described (solid line in Fig. 2). At the same time, the theory cannot account for the constant rate at lower potentials, which must be due to a different process that prevails as the adatom-mediated decay becomes negligible at low potentials.

At present, we can only speculate about the nature of the small, seemingly potential independent rate. Within the framework of our model, one would conclude that for this process the dipole moment in the activated state should be small. Transport by vacancies or by adatoms via exchange diffusion can be excluded because the large dipole moments of the relevant transition states [28] would cause a strong potential dependence of the decay rate. Transport through the substrate surface layer, which is on the verge of reconstruction and thus susceptible to large atom density fluctuations is currently being explored. Such processes have been observed as misfit dislocation glides [31, 32].

6. Discussion

Our theory makes the very general prediction that surface migration rates should vary rapidly with the potential if there is a significant difference in the charge density on surface with and without defects. With respect to the defect-induced shift in the pzc, the rates depend exponentially on the surface charge density, which in turn is roughly proportional to the potential. Concerning the effect of specific adsorption, we have derived an equation that likewise causes rates to change roughly exponentially with the potential. It was shown however that the effect of specific adsorption is small compared to the effect caused by the shift in pzc. Because of its generality, the general prediction of the theory can be tested with experimental data involving surface migration processes even when the details of the underlying atomic processes are not known. Equilibrium fluctuations of steps, e.g., are caused by the migration of atoms along the steps or an exchange of atoms with the terraces and diffusion on the terraces. Step fluctuations on metals in an electrolyte have frequently been found to increase rapidly with the electrode potential, and data have been successfully described by postulating an exponential dependence of the magnitude of the fluctuations on the potential [8-11]. Unfortunately, the charge density was not measured in these studies. However, given the scattering in the data the observed increase in the magnitude of the fluctuations could presumably also represent an exponential increase with the charge density.

For technical reasons it is not possible to measure decay rates in Ostwald ripening or the magnitude of step fluctuations over several orders of magnitude. This limits the possibilities to bring our model to a stringent test. Hirai et al. [6] have measured the decay rate of multilayer holes and stacks of islands on Au(100) surfaces in 50 mM H_2SO_4. These measurements cover two orders of magnitude in the rates. There is a substantial scattering in the data, up to one order of magnitude for the same potential. We attribute the noise to the fact that in the experiments of Hirai et al. the surface geometry was not controlled so that the measured rates actually correspond to islands or holes of different sizes and in different environment. In their paper, Hirai et al. [6] attempted to model the observed rates by thermodynamic considerations. However, their analysis completely neglects the exponential dependence of the rates on the activation energies (concealed in the factor η_S in their rate equations) and merely focuses on the step line tension, which enters linearly in the decay rate as considered by Hirai et al.. At best, their theory therefore

concerns a marginal side effect. Using our capacitance measurements on the same surface electrolyte system, we have plotted the experimental data of Hirai et al. vs. the charge density. The logarithms of island and hole decay-rates vs. the charge density fit to straight lines, in agreement with our model. Dipole moments of $\mu^{+}_{islands} = 0.014$ eÅ and $\mu^{+}_{holes} = 0.026$ eÅ are obtained, for island and hole decay respectively. Because of the large scattering of the data, the difference between the dipole moments for hole filling and mound decay are barely outside the single σ error limit. The dipole moments obtained from this analysis are much smaller than the dipole moments of adatoms or vacancies but in the range of dipole moments for steps [14, 29, 30]. Multilayer island and hole decay involves interlayer transport, i.e. transport of atoms over step edges in addition to transport on terraces. Crossing the step edge is typically the rate determining step because of the Ehrlich-Schwoebel barrier [33, 34]. The activation energy for interlayer transport is then the sum of the energy to create the diffusing species and the activation energy for crossing a step edge (see e. g. [35]). The measured dipole moments should therefore correspond to the dipole moments of the transition states for interlayer diffusion. The lowest activation energy for interlayer transport is obtained for a concerted motion of two atoms in which the diffusing atom replaces a step edge or a kink atom and the step atom becomes an adatom at the step edge of the new kink atom [36]. In that case, the transition state involves two atoms, none of them protruding far out of the surface. A small dipole moment of the transition state in the realm of step dipole moments is therefore expected. The dipole moments relevant for interlayer transport should therefore be considerably smaller then for intralayer transport, in agreement with experiments.

Hirai et al. [6] observed also an increase in the decay rates for potentials negative of pzc, which can also be fitted to a linear dependence on the charge density. This effect was never observed in experiments concerning only intralayer transport. In the framework of our theory, an increase of the rates with negative charge calls for a negative dipole moment of the relevant species. We have calculated positive dipole moments both for the transitions state of adatoms and vacancies. Intralayer transport should therefore always lead to a rate increase with positive potentials, in agreement with the experimental observations. The situation is different for interlayer transport. If the migrating species are vacancies, then the transition state in the step crossing process involves an atom from a step or kink site filling the vacancy. As the participating atoms are closer to the surface, this transition state may have a negative dipole moment. The experimental results of Hirai et al. would then indicate a transition from adatom to vacancy transport when

going from positive to negative potentials. Since, according to our calculations, the activation energies for vacancy transport on Au(100) are only slightly higher than for adatom transport such a transition would in fact be predicted by the theory.

7. Summary

We have developed a theory, which describes general features of the potential dependence of migration processes on surfaces in contact with an electrolyte, i.e. the process of "electrochemical annealing". The model is in agreement with experimental data on the 2D-Ostwald ripening and consistent with rates observed in interlayer transport. It remains to future studies to explore the quantitative aspects of the theory in relation to specific experiments.

Partial support by the Fond der Chemischen Industrie and by the Deutsche Forschungsgemeinschaft is gratefully acknowledged.

[1] M. S. Zei, G. Ertl, Surf. Sci. 442 (1999) 19.
[2] J. M. Doña, J. González-Velasco, Surf. Sci. 274 (1992) 205.
[3] M. Hidalgo, M. L. Marcos, J. Gonzalez-Velasco, Appl. Phys. Lett. 67 (1995) 1486.
[4] J. J. MartinezJubrias, M. Hidalgo, M. L. Marcos, J. Gonzalez-Velasco, Surf. Sci. 366 (1996) 239.
[5] N. Hirai, H. Tanaka, S. Hara, Appl. Surf. Sci. 130-132 (1998) 505.
[6] N. Hirai, K.-I. Watanabe, S. Hara, Surf. Sci. 493 (2001) 568.
[7] K. Kubo, N. Hirai, T. Tanaka, S. Hara, Surf. Sci. 565 (2004) L271.
[8] M. Giesen, M. Dietterle, D. Stapel, H. Ibach, D. M. Kolb, Proc. Mat Res. Soc. 451 (1997) 9.
[9] M. Giesen, M. Dietterle, D. Stapel, H. Ibach, D. M. Kolb, Surf. Sci. 384 (1997) 168.
[10] M. Giesen, R. Randler, S. Baier, H. Ibach, D. M. Kolb, Electrochim. Acta 45 (1999) 527.
[11] M. Giesen, D. M. Kolb, Surf. Sci. 468 (2000) 149.
[12] H. Ibach, W. Schmickler, Phys. Rev. Lett. 91 (2003) 016106.
[13] W. Schmickler, *Interfacial Electrochemistry*, Oxford University Press, Oxford 1995.
[14] G. Beltramo, M. Giesen, H. Ibach, to be published.
[15] H. Ibach, M. Giesen, W. Schmickler, J. Electroanal. Chem. 544 (2003) 13.
[16] Z. Shi, J. Lipkowski, M. Gamboa, P. Zelenay, A. Wieckowski, J. Electroanal. Chem. 366 (1994) 317.
[17] K. Morgenstern, G. Rosenfeld, G. Comsa, Phys. Rev. Lett. 76 (1996) 2113.
[18] K. Morgenstern, G. Rosenfeld, E. Laegsgaard, F. Besenbacher, G. Comsa, Phys. Rev. Lett. 80 (1998) 556.
[19] G. Schulze-Icking-Konert, M. Giesen, H. Ibach, Surf. Sci. 398 (1998) 37.
[20] A. S. Dakkouri, M. Dietterle, D. M. Kolb, Advances in Solid State Physics 36 (1997) 1.
[21] S. Dieluweit, M. Giesen, J. Phys.:Cond. Mat. 14 (2002) 4211.
[22] M. Giesen, Prog. Surf. Sci. 68 (2001) 1.

[23] J. B. Hannon, C. Klünker, M. Giesen, H. Ibach, N. C. Bartelt, J. C. Hamilton, Phys. Rev. Lett. 79 (1997) 2506.
[24] C. Klünker, J. B. Hannon, M. Giesen, H. Ibach, G. Boisvert, L. J. Lewis, Phys. Rev. B 58 (1998) R7556.
[25] S. Dieluweit, H. Ibach, M. Giesen, Faraday Discussions. 121 (2002) 27.
[26] J. E. Müller, Surf. Sci. 178 (1986) 589.
[27] P. J. Feibelman, Phys. Rev. Lett. 65 (1990) 729.
[28] J. E. Müller, H. Ibach, (to be published).
[29] J. Lecoeur, J. Andro, R. Parsons, Surf. Sci. 114 (1982) 320.
[30] A. Hamelin, L. Stoicoveciu, L. Doubova, S. Trasatti, Surf. Sci. 201 (1988) L498.
[31] J. d. l. Figuera, K. Pohl, O. R. d. l. Fuente, A. K. Schmid, N. C. Bartelt, C. B. Carter, R. Q. Hwang, Phys. Rev. Lett. 86 (2000) 3819.
[32] M. Labayen, W. Ramirez, W. Schattke, O. M. Magnussen, Nature Materials 2 (2003) 783.
[33] G. Ehrlich, F. G. Hudda, J. Chem. Phys. 44 (1966) 1039.
[34] R. L. Schwoebel, E. J. Shipsey, J. Appl .Phys. 37 (1966) 3682.
[35] M. Giesen, H. Ibach, Surf. Sci. 431 (1999) 109.
[36] P. J. Feibelman, Phys. Rev. Lett. 81 (1998) 168.